

Binding of More Than One Retinoid to Visual Opsins

Clint L. Makino,^{†*} Charles K. Riley,[‡] James Looney,[†] Rosalie K. Crouch,[§] and Tetsuji Okada[‡]

[†]Department of Ophthalmology, Massachusetts Eye and Ear Infirmary and Harvard Medical School, Boston, Massachusetts;

[‡]Department of Life Science, Gakushuin University, Tokyo, Japan; and [§]Department of Ophthalmology, Medical University of South Carolina, Charleston, South Carolina

ABSTRACT Visual opsins bind 11-*cis* retinal at an orthosteric site to form rhodopsins but increasing evidence suggests that at least some are capable of binding an additional retinoid(s) at a separate, allosteric site(s). Microspectrophotometric measurements on isolated, dark-adapted, salamander photoreceptors indicated that the truncated retinal analog, β -ionone, partitioned into the membranes of green-sensitive rods; however, in blue-sensitive rod outer segments, there was an enhanced uptake of four or more β -ionones per rhodopsin. X-ray crystallography revealed binding of one β -ionone to bovine green-sensitive rod rhodopsin. Cocrystallization only succeeded with extremely high concentrations of β -ionone and binding did not alter the structure of rhodopsin from the inactive state. Salamander green-sensitive rod rhodopsin is also expected to bind β -ionone at sufficiently high concentrations because the binding site is present on its surface. Therefore, both blue- and green-sensitive rod rhodopsins have at least one allosteric binding site for retinoid, but β -ionone binds to the latter type of rhodopsin with low affinity and low efficacy.

INTRODUCTION

The act of seeing begins with photon capture by visual pigments within the rods and cones of the retina. A visual pigment consists of a seven-transmembrane-helix receptor opsin protein, to which the ligand, 11-*cis* retinal (A1) or 3-dehydro 11-*cis* retinal (A2), is bound covalently. Photoexcitation isomerizes the retinal chromophore to the all *trans* conformation, transforming the visual pigment into a catalytically active state that sets off a G protein cascade. Later, all *trans* retinal dissociates from the opsin and is reduced to retinol by a dehydrogenase. Retinol moves from rods and cones to neighboring epithelial cells, is converted to 11-*cis* retinal, and then returns to the photoreceptors to unite with apo-opsin and regenerate rhodopsin, completing the visual cycle. In a second visual cycle pathway, Müller cells produce 11-*cis* retinol, which cones but not rods oxidize to 11-*cis* retinal to regenerate their visual pigment (reviewed in Lamb and Pugh (1) and Travis et al. (2)).

Besides their role in photoreception, retinoids have other effects. High levels are toxic. Retinal can be oxidized to retinoic acid, a transcriptional regulator. Retinoids inhibit the light-regulated channel of photoreceptors (3) and stimulate the catalytic activity of some opsins (4,5). These latter two targets may modulate the overall sensitivity of rods and cones. The ability of a truncated retinal analog, β -ionone, to competitively inhibit the binding of 11-*cis* retinal to opsin led to the proposal that the chromophore-binding pocket of opsin includes a recognition site for the ionone ring (6,7). Yet all *trans* retinal stimulates the catalytic activity of opsin (8) but does not compete with 11-*cis* retinal

for the chromophore-binding pocket (7). In addition, β -ionone increases the catalytic activity of some visual pigments, in which the chromophore-binding pocket is already occupied (9). Accumulating evidence suggests that rod opsin bears more than one binding site for retinoids (reviewed in Heck et al. (10)). Here we investigate the issue using β -ionone. Binding of β -ionone to rhodopsin in green-sensitive rods (GSRs) and blue-sensitive rods (BSRs) of salamander would increase their UV absorbance, so uptake was measured by single cell microspectrophotometry. Localization of β -ionone binding to bovine rhodopsin was determined by x-ray crystallography. Some results have appeared in abstract form (11).

METHODS

X-ray crystallography

β -Ionone (Sigma Chemical, St. Louis, MO) was purified by double distillation, diluted in ethanol, and included in the mother liquor in excess over rhodopsin while keeping other conditions similar to those reported previously (12). Briefly, the solution of β -ionone in ethanol was diluted 240-fold with the rhodopsin solution prepared for crystallization as before (12). Two representative data sets (3.5 mM and 7 mM β -ionone) were collected at BL41XU of SPring-8, Hyogo, Japan. Such high concentrations of β -ionone appeared necessary to maintain the bound state because we could not confirm the binding in crystals grown with [β -ionone] = 0.5 or 1.1 mM. The data sets were processed with HKL2000 (13), and binding of β -ionone was confirmed by calculating the difference maps between the two data sets and the native (β -ionone minus) data sets using the phases from the previously obtained rhodopsin structure (PDB ID: 1U19). Because the appearance of the electron densities was better for data set 1, a β -ionone molecule was placed manually in each of the two rhodopsin models in the asymmetric unit obtained with that set and refined further with CNS (14). The refined model was validated (Ramachandran zone distribution: 81.5/13.2/3.6/1.7) using PROCHECK (15). The outliers are similar to those in the rhodopsin-only model and most of them are in the third cytoplasmic loop or in the carboxyl terminal tail.

Submitted July 6, 2010, and accepted for publication August 4, 2010.

*Correspondence: cmakino@meei.harvard.edu

Editor: Axel T. Brunger.

© 2010 by the Biophysical Society
0006-3495/10/10/2366/8 \$2.00

doi: 10.1016/j.bpj.2010.08.003

Microspectrophotometry

Retinas from the tiger salamander, *Ambystoma tigrinum*, were removed under infrared illumination after dark adaptation of an animal overnight, and shredded on a quartz coverslip previously coated with poly-L-lysine. Double-sided tape lined two opposing edges and a second coverslip was placed on top. This sandwich-type chamber was mounted on the stage of the Williams-Webbers microspectrophotometer (16). Baseline measurements were taken with the polarized probe beam passing through a cell free area. The beam was then positioned on a cell with its electric vector oriented perpendicular to the long axis of the outer segment (\perp). Some outer segments were rotated 90° for a second measurement (\parallel). Measurements were made at room temperature: 21–23°C.

Individual rods (see the Supporting Material) contained mixed pigment populations, wherein the opsin bound either an A1 or an A2 chromophore (17). The A2 visual pigment has a longer wavelength absorbance maximum and reduced extinction, compared to its A1 counterpart. The absorbance of each component was determined by fitting spectra with the sum of A1 and A2 templates (18), assuming A1 and A2 pigment maxima at 501 nm and 519 nm in GSRs and at 428 nm and 435 nm in BSRs, respectively. The fractional composition was determined using extinction coefficients: $\epsilon_{A1} = 42,000 \text{ M}^{-1} \text{ cm}^{-1}$ and $\epsilon_{A2} = 30,000 \text{ M}^{-1} \text{ cm}^{-1}$ (19,20). For GSRs in this study, A2 content ranged from 44% to 100% in aquatic salamanders and from 23% to 82% in terrestrial salamanders. Mean values are collected in Table 1. In control experiments on nine GSRs, OD_{\perp} measurement bleached $0.14 \pm 0.09\% \text{ scan}^{-1}$ (mean \pm SE) of the A2 component and $0.22 \pm 0.15\% \text{ scan}^{-1}$ of the A1 component. Combined bleaches of up to 10% were considered to be acceptable.

Ringer's contained: 108 mM NaCl, 2.5 mM KCl, 1.0 mM MgCl_2 , 10 mM HEPES, 1.5 mM CaCl_2 , 0.02 mM EDTA, 10 mM glucose, and in some experiments, 0.7 μM bovine serum albumin (BSA, Fraction V, γ -globulin-free, or fatty acid free, Sigma); pH 7.6. β -Ionone in an ethanolic solution was diluted with Ringer's, keeping [ethanol] $<0.15\%$. The final [β -ionone] was confirmed spectrophotometrically, using $\epsilon_{\beta} = 8700 \text{ M}^{-1} \text{ cm}^{-1}$. β -Ionone was perfused through the chamber, two to four times in rapid succession. Because it was not always possible to measure absorbance before and after treatment in the same rod, the average for each condition derived from overlapping populations of cells. In control experiments to determine the bleach due to scanning, the Ringer's contained 5 mM

NH_2OH (Sigma), to prevent spectral interference by long-lived photointermediates.

In spectra obtained from rhodopsin crystals, absorbance was sometimes so high that there were distortions due to nonlinearity in the instrument. OD values exceeding 1.1 were therefore deleted and spectra with very broad bandwidth were rejected. In control experiments on two crystals, the bleaching rate per scan was $<0.2\%$. Absorbance maxima of the main rhodopsin band were determined from fits of spectra in which $<5\%$ of the rhodopsin had been bleached, with a fourth-order polynomial for $OD > 0.8$ of the maximum (Igor Pro v. 5.03; Wavemetrics, Lake Oswego, OR). For all other analyses, a bleach of $<10\%$ was deemed acceptable.

RESULTS

Uptake of β -ionone into rods determined by microspectrophotometry

Perfusion of GSRs with β -ionone increased their ultraviolet (UV) absorbance (Fig. 1). Baseline measurements were made with β -ionone present in the bathing solution so the spectral change indicated an accumulation of the substance within the cells. The time course of the absorbance change was not resolved because uptake equilibrated in $<5 \text{ min}$ —within the time taken to deliver the β -ionone. There was uptake into the ellipsoid (not shown), an area densely packed with mitochondria (21), as well as into the outer segment, where all of the rhodopsin is localized. For five GSRs bathed in 347 μM β -ionone, the ratio of uptake into the outer segment to that in the ellipsoid area of the inner segment was 1.2.

The molar ratio of β -ionone to visual pigment in the outer segment was estimated as

$$\beta/\text{Rh} = \frac{(1.5)(OD_{\beta}/\epsilon_{\beta})}{OD_{A1}/\epsilon_{A1} + OD_{A2}/\epsilon_{A2}}, \quad (1)$$

where OD_{β} is the absorbance attributed to β -ionone from the difference spectrum, OD_{A1} and OD_{A2} are the absorbances of the A1 and A2 components of the visual pigment from a template fit, and the ϵ -values are the extinction coefficients for each component in solution. The factor of 1.5 accounts for rhodopsin dichroism in situ. The experiments yielded difference spectra whose spectral position varied from $\sim 270 \text{ nm}$ to 305 nm . Peaks $\leq 280 \text{ nm}$ were encountered at low bathing [β -ionone] where the amplitudes were sometimes negative (UV absorbance was lower in cells treated with β -ionone). Those cases reflected slight variability in the ratio of the protein/visual pigment absorbance rather than a difference in β -ionone content. In Fig. 1, the absorbance of treated and untreated rods matched nearly perfectly over the range from 400 to 650 nm. More often, there were small mismatches, so the untreated rod spectrum was corrected by a multiplicative factor, before taking the difference spectrum.

In four experiments with [β -ionone] ranging from 30 to 90 μM , the mean ratio of uptake into the outer segments of intact GSRs versus that into detached GSR outer segments that lacked mitochondria was 1.02, indicating

TABLE 1 Spectral features of GSRs and BSRs

	GSR	BSR	<i>p</i> -value
Visual pigment			
OD_p/OD_{Rh}	$1.79 \pm 0.05, 23$	$2.11 \pm 0.24, 9$	ns
%A2	$77 \pm 7, 13$	$65 \pm 6, 13$	ns
Dichroic ratio	$3.06 \pm 0.06, 20$	$2.42 \pm 0.10, 7$	$9e-6$
β -ionone			
λ_{max}, nm	$296 \pm 1, 12$	$291 \pm 1, 6$	0.004
<i>w</i> , nm	$40 \pm 1, 12$	$42 \pm 4, 6$	ns
Dichroic ratio	$1.04 \pm 0.05, 10$	$1.06 \pm 0.05, 3$	ns

Mean \pm SE, *n* for GSR parameters derived from average values of many rods in an experiment, where *n* is the number of experiments; ns, not significant. BSR results were analyzed only when there were two or more cells measured per experiment. OD_p/OD_{Rh} is the ratio of the absorbance for the protein band near 280 nm to that for the main rhodopsin band. %A2 gives the percentage of A2 pigment based on template fits for experiments with GSR and BSR results from the same salamander. β -Ionone parameters were estimated from difference spectra as shown in Figs. 1 and 3 in which [β -ionone] in the bath was $\geq 30 \mu\text{M}$. The full bandwidth at half-height of the difference spectrum is given by *w*. Dichroic ratio = $OD_{\perp}/OD_{\parallel}$ for rhodopsin and for β -ionone at their spectral maxima. Before calculating the dichroic ratio of β -ionone in BSRs, absorbance due to bulk uptake of β -ionone, as estimated from the relation for GSRs (Fig. 1 B), was subtracted from the numerator and from the denominator.

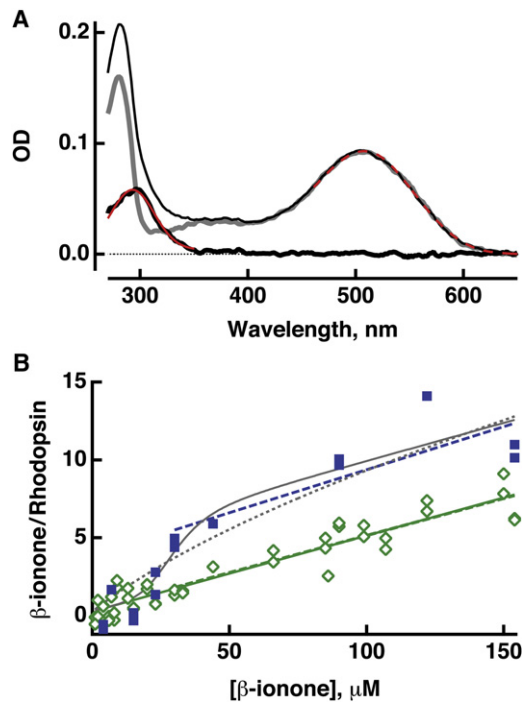


FIGURE 1 β -Ionone uptake into rod outer segments. (A) Subtraction of the average absorption spectrum (OD_{\perp} ; see Methods) of 10 untreated GSRs (thick gray line) from that of 16 GSRs treated with $66 \mu\text{M}$ β -ionone (thin black line) yielded a difference spectrum (thick black line) with a peak at 292 nm (Gaussian fit, red line). After a template fit of the untreated GSR spectrum (dashed red line) to determine the rhodopsin content, the β /Rh ratio was estimated to be 3.2 (see text). (B) Linear regression of β -ionone uptake as a function of $[\beta\text{-ionone}]$ in the bath for GSRs (green diamonds) yielded a slope = $0.049 \mu\text{M}^{-1}$ and a y intercept = 0.26 (continuous green line). For $[\beta\text{-ionone}] \geq 30 \mu\text{M}$ (dashed green line), the slope = $0.048 \mu\text{M}^{-1}$ and y intercept = 0.38. For BSRs (blue squares), linear regression for $[\beta\text{-ionone}] \geq 30 \mu\text{M}$ (dashed blue line) returned a slope of $0.055 \mu\text{M}^{-1}$ and an intercept of 3.84. Fitting all BSR results with a Michaelis-Menten function summated with the linear relation obtained for GSRs (dotted gray line) suggested that eight molecules of β -ionone bound at saturation, K_m near $90 \mu\text{M}$. Substituting a Hill function for the Michaelis-Menten produced a slightly better fit (continuous gray line) with a Hill coefficient of 4.8 and K_m of $30 \mu\text{M}$. β -Ionone uptake was determined from OD_{\perp} and OD_{\parallel} measurements, whereas pigment content was taken from OD_{\perp} measurements. For some experiments with low bathing concentrations of β -ionone, the Gaussian fit to the difference spectrum was poor, so uptake was evaluated as the mean absorbance of the difference spectrum between 285 and 300 nm minus that between 350 and 365 nm.

that the accumulation did not require a cellular energy source. Measurements of each type were therefore pooled in all experiments. Inclusion of $0.7 \mu\text{M}$ BSA in the Ringer's to facilitate delivery of β -ionone had little or no effect on the results. Uptake of β -ionone increased in proportion to its bath concentration, attaining β /Rh ratios that surpassed 7 (Fig. 1 B). These observations accord with the avid partitioning of a hydrophobic molecule into membranes. Assuming $[\text{rhodopsin}] \approx 3.3 \text{ mM}$ in the outer segment (22), the slope of the concentration dependence of uptake implied a partition ratio of $(0.049 \mu\text{M}^{-1})/(3300 \mu\text{M}) = 162$. At low bathing $[\beta\text{-ionone}]$, minor variability in

measurements of the protein absorbance introduced scatter in the determination of uptake; however, restricting the analysis to $[\beta\text{-ionone}] \geq 30 \mu\text{M}$ did not alter the slope or intercept of the uptake relation appreciably. Because a nonzero y intercept would obtain if β -ionone bound to rhodopsin, these results preclude specific binding of even a single β -ionone to rhodopsin in GSRs with very low K_m .

Visual pigments orient in the disk-membranes such that light absorption is optimal with the electric vector of the measuring beam aligned perpendicular to the long axis of the outer segment (OD_{\perp}). The absorbance measured in this configuration, divided by that with the rod oriented orthogonally (OD_{\parallel}), yielded a dichroic ratio of 3.1 (Table 1), comparable to a previous report (22). In contrast, the mean dichroic ratio for β -ionone was 1.0 with little evidence for any dependence on bathing concentration. The absence of dichroism provided further support for membrane partitioning, given that β -ionone distributes randomly throughout different depths of the lipid bilayer (23).

Washing GSRs with Ringer's containing BSA after treatment with $33 \mu\text{M}$ β -ionone removed $>90\%$ of the β -ionone (Fig. 2), matching the reversibility reported in physiological experiments (4,5,9). As with uptake, washout occurred rapidly, within the period of time elapsing for chamber perfusion. However, after treatment with 50 – $150 \mu\text{M}$ β -ionone, 25 – 55% of the β -ionone was retained, even after more than one wash, for at least 2 h.

The binding pocket for 11-*cis* retinal in opsin accommodates β -ionone (6,7), so to demonstrate that our method could detect pocket occupancy, the β -ionone content was followed in nine GSRs as they were treated with $107 \mu\text{M}$ β -ionone, washed with BSA, bleached, washed with BSA again, and finally treated with β -ionone a second time (data not shown). The initial exposure to β -ionone produced a β /Rh of 4.6. Washout was incomplete; β /Rh dropped to 1.0. After bleaching, the second treatment with β -ionone increased β /Rh to 5.5, presumably by allowing one β -ionone

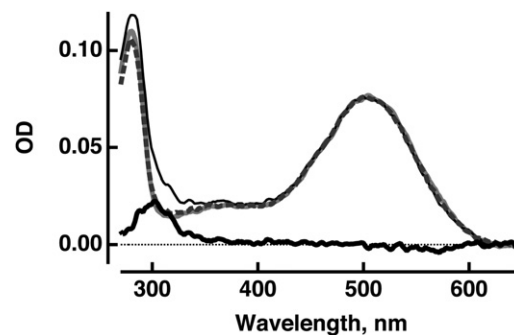


FIGURE 2 Washout of β -ionone. Seventeen GSRs were treated with $33 \mu\text{M}$ β -ionone (thin black line). Subtraction of the scaled spectrum of 21 untreated GSRs (continuous gray line) gave a difference spectrum revealing the extent of uptake (thick black line). Perfusion with Ringer's containing BSA removed nearly all of the β -ionone from the 17 GSRs (broken gray line).

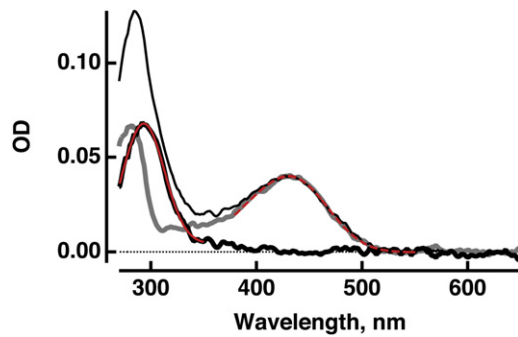


FIGURE 3 Enhanced uptake of β -ionone into BSRs. The difference spectrum (thick black line) was obtained by subtracting the average absorption spectrum (OD_{\perp}) from three untreated cells (thick gray line) from the spectrum of five cells treated with $90 \mu\text{M}$ β -ionone (thin black line). The Gaussian fit (continuous red line) yielded a spectral maximum at 293 nm. β/Rh was 9.7.

molecule to reside in the vacant chromophore-binding pocket of opsin.

Blue-sensitive rods were encountered far less frequently. The visual pigment in BSRs had a lower dichroic ratio than that of GSRs (22). Although the difference spectra for BSRs and GSRs had very similar spectral bandwidths, there was a slight shift in the maximum for BSRs to shorter wavelength (Figs. 1 and 3; Table 1). In addition, β/Rh was, on average, 2.1-fold greater for BSRs, once $[\beta\text{-ionone}]$ in the bath reached $30 \mu\text{M}$ or more. The greater relative amplitude could not be attributed to preferential alignment of β -ionone molecules parallel to the measuring beam because there was no systematic pattern of dichroism in BSRs with β -ionone concentration. Regression analysis of BSR uptake at $[\beta\text{-ionone}] \geq 30 \mu\text{M}$ yielded a slope similar to that obtained for GSRs, but with a y intercept near 4. Fitting all BSR results with the linear relation obtained for GSRs plus a Michaelis-Menten relation for independent binding to sites with equal affinity provided a crude estimate of eight binding sites with K_m near $90 \mu\text{M}$ (dotted gray line, Fig. 1 B). If binding were cooperative, then five β -ionone molecules may have bound with a K_m of $\sim 30 \mu\text{M}$ (continuous gray line, Fig. 1 B). Although the data do not draw a distinction between the various models, all of them are consistent with the binding of several β -ionones to BSR rhodopsin.

Cocrystallization of rhodopsin with β -ionone

Despite the lack of evidence for binding to the rhodopsin in salamander GSRs, cocrystallization of bovine GSR rhodopsin with millimolar β -ionone proved to be successful. Crystals were subjected to microspectrophotometry to corroborate the presence of β -ionone. P4_1 crystals of rhodopsin alone (Ro) exhibited an absorbance maximum of $492.9 \pm 0.5 \text{ nm}$ (mean \pm SE, $n = 9$ measurements on five crystals), somewhat blue-shifted from the 498 nm for bovine rhodopsin in solution, though reminiscent of the P3_1 crystal spectrum (24). The spectral maximum for P4_1 crystals of

rhodopsin plus β -ionone ($\text{R}\beta$) was similar, $491.7 \pm 0.5 \text{ nm}$ (six measurements on four crystals). In addition, the main absorption band for both types of crystals was broad, conforming more closely to an A2 rather than an A1 template (18). These attributes may have arisen from photoexcitation of some of the rhodopsin by red light used for evaluating crystal growth and for manipulating the crystal during sample preparation. As expected from previous descriptions of P4_1 crystals of rhodopsin (12,25), absorption by the rhodopsin band was optimal with the electric vector of the measuring beam oriented orthogonally to the long axis of the crystal (Fig. 4, A–C). For very large crystals, the maximal absorbance of the main pigment band was estimated by fitting both sides of the peak with a template, disregarding the high absorbance values which were subject to nonlinearity in measurement. The highest dichroic ratios were then 2.9 for an Ro crystal and 3.7 for an $\text{R}\beta$ crystal. The mean dichroic ratios were: 2.0 ± 0.5 for five Ro crystals and 2.9 ± 0.3 for six $\text{R}\beta$ crystals, with 1–3 determinations made per crystal. The difference in dichroism, although statistically significant, probably reflected distortion of crystals during sample preparation rather than the presence of β -ionone. There was also a secondary maximum near 330 nm in OD_{\parallel} spectra (Fig. 4 B). This feature, which was not observed in absorption spectra of intact rods (22), may be a better resolution of the *cis* peak due to greater homogeneity in bond angles within 11-*cis* retinal and alignment of partial chromophores (26) perpendicular to the long axis of the crystal. The relatively large size of the secondary maximum shifted the peak of the main band in OD_{\parallel} spectra to slightly shorter wavelength: $489.2 \pm 0.7 \text{ nm}$ for Ro (14 measurements on five crystals) and $487.7 \pm 0.7 \text{ nm}$ for $\text{R}\beta$ crystals (13 measurements on seven crystals).

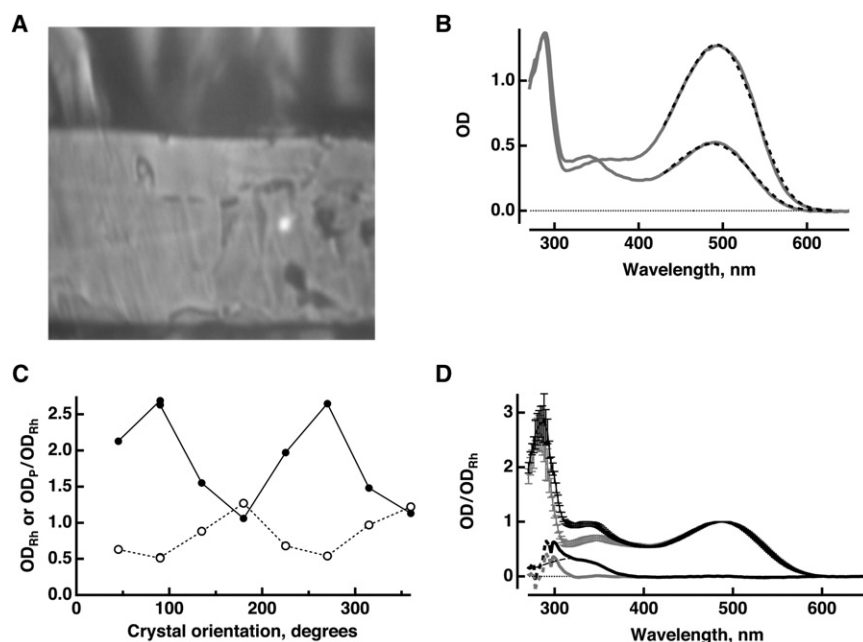
The presence of β -ionone in $\text{R}\beta$ crystals was indicated by a higher absorbance near 290 nm (Fig. 4 D). With spectra taken away from the dichroic maximum of the main rhodopsin band, there was a larger secondary maximum for $\text{R}\beta$ than for Ro crystals, a feature presumed to be related to the higher dichroic ratio of $\text{R}\beta$. The contribution of the secondary maximum was removed before estimating the molecular ratio of β -ionone to rhodopsin (e.g., Fig. 4 D) at orthogonal orientations of the crystals as

$$\text{Horizontal} \quad \beta/\text{Rh} = (\epsilon_{A1})(\widehat{OD}_{\beta})/(\epsilon_{\beta} \sin\theta) = 0.4, \quad (2)$$

$$\text{Vertical} \quad \beta/\text{Rh} = (\epsilon_{A1})(\widehat{OD}_{\beta})/(D\epsilon_{\beta} \cos\theta) = 1.5, \quad (3)$$

where $\widehat{OD}_{\beta} = OD_{\beta}/OD_{\text{Rh}}$, $D = 2.9$ is the mean dichroic ratio for $\text{R}\beta$ crystals and θ is 63.5° (the angle of the vector drawn from the aldehyde group of β -ionone to C5 in the ring relative to the long axis of the crystal). The mean of the two estimates was 0.9, denoting that a single β -ionone was bound to each rhodopsin molecule.

Specific binding was confirmed by solving the x-ray crystallographic structure for $\text{R}\beta$ (Fig. 5). The space group,



bars). A spectral component absorbing near 330 nm (dashed black line) was removed to reveal the absorbance of β -ionone in isolation (thick continuous gray line). Values near 280 nm were disregarded due to the limited number of usable observations (hence large SEs in the Ro and R β spectra).

lattice constants, and arrangement of the helices were nearly the same as for Ro crystals, making it possible to use the previously solved crystal structure of rhodopsin at 2.2 Å (12) to better define the features attributable to β -ionone. Parameters for the crystals are summarized in Table 2. Electron density corresponding to β -ionone was discovered near the third extracellular loop connecting helices VI and VII in both data sets 1 and 2. Each rhodopsin had a β -ionone bound to the site; occupancy refinement with data set 1 yielded values of 0.96 and 0.91 for the pair of rhodopsins comprising the asymmetric unit. A hairpin structure of the Gly-Pro-Ile-Phe residues 284–287 formed the binding site. The interaction between the cyclohexenyl ring and the opsin moiety was predominantly hydrophobic. Other residues in the vicinity that may contribute to binding include V271, D282, F283, and I290. No specific interaction was found for the aldehyde group of β -ionone with rhodopsin. Locating β -ionone into this site displaced only a single

water molecule in the 2.2 Å structure model (12). The arrangement of the helical segments of rhodopsin, helices III and VI in particular, were unchanged by the presence of β -ionone.

DISCUSSION

Visual opsins are G-protein-coupled receptors for retinoids whose low basal catalytic activity is quenched by the covalent binding of 11-*cis* retinal as it regenerates rhodopsin. Light isomerizes 11-*cis* retinal to the all-*trans* conformation, converting an inverse agonist to a full agonist. Other retinoids lacking the full polyene side chain and/or the terminal aldehyde moiety do not bind covalently and their identity as agonist or inverse agonist is dependent upon opsin type (4,5,27,28). For example, β -ionone extinguishes the activity of red-sensitive cone (RSC) opsin but stimulates the activities of blue- (BSC) and UV-sensitive cone (UVSC)

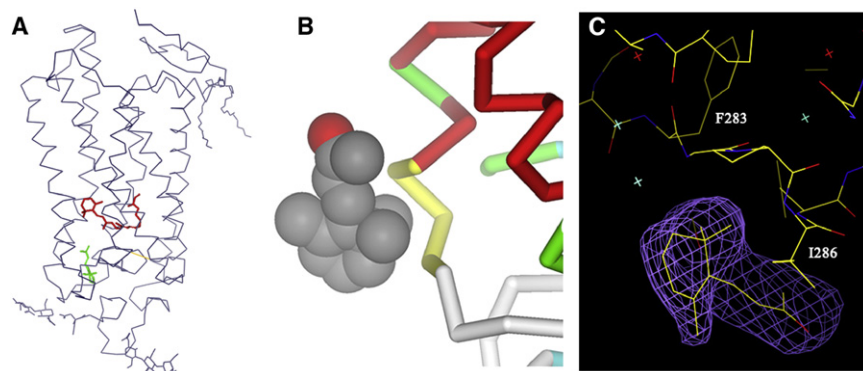


FIGURE 5 Structure of bovine rhodopsin with β -ionone bound. (A) 11-*cis* retinal + K296 (red), β -ionone (green), and disulfide bond between C110 and C187 (orange line). (B) β -ionone (space-filled) docked onto rhodopsin (yellow, residues 284–287; red, a part of transmembrane helix; green, irregular helical region; white, extracellular loop). (C) A simulated-annealed omit map was calculated using the structure factor amplitudes from an R β crystal (7.0 mM β -ionone, data set 1) and phases from the model excluding β -ionone and nearby region within 2.5 Å. The map was contoured at the 4 σ level.

TABLE 2 Crystallographic data collection and refinement statistics of the rhodopsin- β -ionone complex

	Data set 1	Data set 2
Data collection		
Resolution range, Å	50–2.6	50–2.9
Unit cell ($a = b, c$), Å*	96.99, 149.8	97.18, 150.0
Twin fraction	0.017	0.041
Mosaicity, °	0.326	0.613
Total observations	185,254	133,902
Unique observations	39,801	28,156
R_{merge} , % (outer shell)	9.50 (50.4)	11.1 (59.0)
Completeness, % (outer shell)	93.6 (67.9)	91.3 (51.1)
$I/\sigma(I)$, (outer shell)	14.1 (1.56)	11.9 (1.57)
Wilson B factor, Å ²	60.7	70.6
Refinement		
R_{cryst}	22.5	
R_{free}	26.2	
RMSD bonds	0.008	
RMSD angles	1.24	
Occupancy (β -ionone)	0.96, 0.91	

$$R_{\text{merge}} = \frac{\sum_{\text{hkl}} \sum_i |I_i(\text{hkl}) - \langle I(\text{hkl}) \rangle|}{\sum_{\text{hkl}} \sum_i I_i(\text{hkl})}$$

$R_{\text{cryst}} = \frac{\sum_{\text{hkl}} |F_o - F_c|}{\sum_{\text{hkl}} |F_o|} \cdot R_{\text{free}}$ was calculated from a set of 5% randomly selected reflections that were omitted from refinement.

*Space group is P4₁.

opsins and GSR opsin. Because many retinoids slow the rate of pigment regeneration with 11-*cis* retinal (6,7,29,30), their effects on catalytic activity are thought to be mediated by binding to a common site (27). However, all *trans* retinal is an agonist for opsin that accelerates slightly the rate of GSR pigment regeneration by 11-*cis* retinal (31). Moreover, in physiological experiments, β -ionone remained an effective agonist for BSR/BSC opsin and for UVSC opsin even after the chromophore-binding pocket was filled by regenerating the pigment (9). Although β -ionone has little efficacy for GSR visual pigment, retinol is an agonist ((11), see also (32)). In explanation, small hydrophobic molecules such as retinoids incorporate into the bilayer and by changing its physical properties, could alter the activities of integral membrane proteins (reviewed in Andersen and Koeppe (33) and McIntosh and Simon (34)). A more intriguing possibility, not mutually exclusive, is that opsins possess more than one retinoid binding site. Allosteric modulation has been described for many other G-protein-coupled receptors (reviewed in Wang et al. (35)). Because retinoid binding to visual pigment leaves a spectral signature, single rods were probed by microspectrophotometry before and during exposure to β -ionone. Physiological experiments failed to show visual pigment activation in salamander GSRs at $[\beta\text{-ionone}] < 60 \mu\text{M}$ (9), so measurements on these cells were included to distinguish lack of binding from lack of efficacy.

When added to the bath, β -ionone incorporated rapidly into the outer segment and ellipsoid of GSRs without any specific binding to rhodopsin. Uptake into BSRs matched that in GSRs at low bath concentrations of β -ionone, but at higher concentrations, uptake incremented by four or more β -ionones per rhodopsin.

Two considerations were ruled out before inferring that there were binding sites for β -ionones on the BSR rhodopsin.

First, the lipid composition of gecko photoreceptor outer segment membranes deviates from that of frog and bovine rods perhaps because cone pigments require a different lipid environment than rod pigments (36). BSRs express a cone pigment (37), so if their outer segment lipids differ from those in GSRs, β -ionone may partition more completely in BSR membranes. But then uptake would increase in greater proportion to bathing concentration for BSRs than for GSRs. Our observations indicated otherwise; at bath concentrations $\geq 30 \mu\text{M}$, the intercept of the linear relation for BSRs was displaced from the origin and the slope did not differ significantly from that for GSRs (Fig. 1 B).

Second, β -ionone bleaches BSR rhodopsin, albeit at a very slow rate (9). BSRs were usually measured within minutes after application of β -ionone to minimize the extent of bleach. Some apo-opsin could have been present even before treatment with β -ionone because pigment regeneration in BSRs is often incomplete, even after extensive dark adaptation of salamanders (9,38). Dividing the absorbance due to β -ionone in the membrane plus that residing in the chromophoric binding pocket of opsin by the absorbance of a less-than-full complement of rhodopsin would then give a spuriously high uptake ratio. However, the amount of free opsin would have to have been equal to or greater than the amount of pigment in order to explain the high β/Rh observed in BSRs. Another argument may be advanced as follows. GSR opsin has five tryptophans and 21 tyrosines, whereas BSR opsin has seven and 13, respectively (39,40). Assuming extinction coefficients of $5690 \text{ M}^{-1} \text{ cm}^{-1}$ for tryptophan and $1280 \text{ M}^{-1} \text{ cm}^{-1}$ for tyrosine at 280 nm (41), BSR and GSR opsins absorb similarly at 280 nm. Because rod and cone rhodopsins have very similar extinction coefficients at their absorbance maxima (42–45), the ratio of absorbance near 280 nm to that at λ_{max} was used to gauge rhodopsin content. The ratios for GSRs and BSRs were similar (Table 1), supporting the notion that the bleached visual pigment content was low in BSRs. Given that physiological experiments demonstrated activation of rhodopsin and the phototransduction cascade by β -ionone in intact, dark-adapted BSRs and BSCs as well as in UVSCs (9), we conclude that the enhanced uptake of β -ionone into BSRs arose at least in part from binding to the visual pigment.

Cascade activation in BSRs was saturated at bath concentrations of $\sim 10 \mu\text{M}$ β -ionone (9). Uptake measurements suggest that only one or two β -ionones bound each rhodopsin under those conditions (Fig. 1 B). The mechanism of action is not known. Because β -ionone also caused pigment bleaching, it could lower the activation energy of the visual pigment and accelerate the rate of thermal isomerization. Alternatively, β -ionone could stabilize the active conformation of the visual pigment with pigment bleaching

as a secondary consequence. RSC pigment will transfer its 11-*cis* retinal chromophore to GSR opsin (46) or to a retinal binding protein, CRALBP (38) without isomerization. The rate of chromophore release by RSC pigment is accelerated by the presence of β -ionone (9) or 9-*cis* retinal (38,46). Thus, a third possibility is that binding of β -ionone(s) near the chromophore binding pocket of opsin (Fig. 5) simply increases the local concentration of β -ionone, enabling it to compete with and more effectively displace the native chromophore.

After finding that β -ionone failed to bind (this study) or activate (9) salamander GSR rhodopsin, it was surprising to discover that β -ionone incorporated into the crystal structure of bovine GSR rhodopsin. A species difference between bovine and salamander rhodopsins seems unlikely, given that the residues 284–287 in bovine rhodopsin that interact with the ring portion of β -ionone are absolutely conserved in salamander GSR rhodopsin. The binding sequence, GPxF where *x* is either I or V, is also present in the GSR opsin of other species (Fig. S1 in the Supporting Material). Among the other residues that may contribute to binding, i.e., V271, D282, F283, and I290, there is an I290V substitution in salamander GSR opsin. We therefore presume that β -ionone binds to all GSR rhodopsins at a site that can only be occupied at exceedingly high salt and/or ligand concentrations. The structure of bovine rhodopsin was unchanged by the binding of β -ionone. In particular, positioning of the sixth helix resembled that in catalytically inactive rhodopsin (12) and differed from that in the partially active opsin (47,48). Thus, in GSR rhodopsin, binding either did not lead to activation or activation was suppressed by crystal lattice contacts.

If the corresponding residues participate in binding β -ionone to BSR rhodopsin, several substitutions could detract from the hydrophobicity of the site, i.e., G284D, P285L, I286R, and F287M, whereas V271F and D282L might enhance it (GSR opsin numbering). P285L also disrupts the hairpin turn. Interestingly, locating β -ionone on the helix 6–7 linker poises it near one of the lower probability sites of retinal egress from GSR suggested by molecular dynamics (49), which may be relevant to its mode of BSR pigment activation. The binding of additional β -ionones to BSR rhodopsin could involve four other proposed retinoid binding sites on GSR rhodopsin. Two sites within opsin, along with the chromophore-binding pocket, form a retinoid channel through the protein (50). The channel-forming sites are not accessible in GSR rhodopsin; however, the situation could differ in BSR rhodopsin. For example, the Schiff base linkage of 11-*cis* retinal to lysine in BSR pigment is vulnerable to chemical attack by hydroxylamine, whereas that in GSR pigment is not (37,51,52). Limited access to the channel in GSR rhodopsin may help to confer its extraordinary thermal stability. Two other potential sites were located on the intracellular surface (53). One site nestles alongside the palmitoylation sites attached to C322 and C323.

Palmitoylation may be important for binding because the activation of bovine GSR opsin by all *trans* retinal decreases upon their removal (31). Both cysteines are conserved in salamander GSR opsin (39). One is conserved in BSR opsin (40), although recombinant BSR protein expressed in COS exhibits heterogeneity in the palmitoylation status (54). There are also sites in GSR rhodopsin crystals occupied by detergent and small amphiphilic molecules (e.g., (55)) that could have a higher affinity for retinoids in BSR rhodopsin. Finally, nonspecific binding of β -ionones to BSR rhodopsin may have been greater than to GSR rhodopsin.

Differences in the allosteric modulation of G-protein coupled receptors sometimes exist between members of a group that share the same orthosteric ligand (35). Thus, in future studies, it will be important to find out how many retinoid binding sites are present on each type of opsin; which retinoids bind to them; under what circumstances they are occupied; and the physiological significance of each site.

SUPPORTING MATERIAL

One figure is available at [http://www.biophysj.org/biophysj/supplemental/S0006-3495\(10\)00969-0](http://www.biophysj.org/biophysj/supplemental/S0006-3495(10)00969-0).

The coordinates and structure factors have been deposited with the accession code 3OAX.

We thank D. Alexeev for carrying out several preliminary experiments.

Supported by grant Nos. NEI EY011358, EY014104, EY019515, and EY04939 from the Lions of Massachusetts, an unrestricted grant to the Department of Ophthalmology at the Medical University of South Carolina from Research to Prevent Blindness (RPB, New York), and Grant-in-Aid for Scientific Research (KAKENHI) grant No. 19370071 from the Ministry of Education, Culture, Sports, Science and Technology of Japan. R.K.C. is an RPB senior scientific investigator.

REFERENCES

- Lamb, T. D., and E. N. Pugh, Jr. 2004. Dark adaptation and the retinoid cycle of vision. *Prog. Retin. Eye Res.* 23:307–380.
- Travis, G. H., M. Golczak, ..., K. Palczewski. 2007. Diseases caused by defects in the visual cycle: retinoids as potential therapeutic agents. *Annu. Rev. Pharmacol. Toxicol.* 47:469–512.
- Dean, D. M., W. Nguitraagool, ..., A. L. Zimmerman. 2002. All-*trans*-retinal shuts down rod cyclic nucleotide-gated ion channels: a novel role for photoreceptor retinoids in the response to bright light? *Proc. Natl. Acad. Sci. USA.* 99:8372–8377.
- Kefalov, V. J., M. C. Cornwall, and R. K. Crouch. 1999. Occupancy of the chromophore binding site of opsin activates visual transduction in rod photoreceptors. *J. Gen. Physiol.* 113:491–503.
- Isayama, T., Y. Chen, ..., C. L. Makino. 2006. Differences in the pharmacological activation of visual opsins. *Vis. Neurosci.* 23:899–908.
- Matsumoto, H., and T. Yoshizawa. 1975. Existence of a β -ionone ring-binding site in the rhodopsin molecule. *Nature.* 258:523–526.
- Daemen, F. J. M. 1978. The chromophore binding space of opsin. *Nature.* 276:847–848.
- Yoshizawa, T., and Y. Fukada. 1983. Activation of phosphodiesterase by rhodopsin and its analogues. *Biophys. Struct. Mech.* 9:245–258.

9. Isayama, T., S. L. McCabe England, ..., C. L. Makino. 2009. β -ionone activates and bleaches visual pigment in salamander photoreceptors. *Vis. Neurosci.* 26:267–274.
10. Heck, M., S. A. Schädell, ..., K. P. Hofmann. 2003. Secondary binding sites of retinoids in opsin: characterization and role in regeneration. *Vision Res.* 43:3003–3010.
11. Isayama, T., T. Okada, ..., C. L. Makino. 2009. An additional retinoid binding site in rhodopsin. 2009 Biophysical Society Meeting Abstracts. *Biophys. J. (Suppl)*, 528a, (Abstract), 2718-Pos.
12. Okada, T., M. Sugihara, ..., V. Buss. 2004. The retinal conformation and its environment in rhodopsin in light of a new 2.2 Å crystal structure. *J. Mol. Biol.* 342:571–583.
13. Otwinowski, Z., and W. Minor. 1997. Processing of x-ray diffraction data collected in oscillation mode. *Methods Enzymol.* 276:307–326.
14. Brünger, A. T., P. D. Adams, ..., G. L. Warren. 1998. Crystallography and NMR system: a new software suite for macromolecular structure determination. *Acta Crystallogr. D Biol. Crystallogr.* 54:905–921.
15. Laskowski, R. A., M. W. MacArthur, ..., J. M. Thornton. 1993. PROCHECK—a program to check the stereochemical quality of protein structures. *J. Appl. Cryst.* 26:283–291.
16. Makino, C. L., L. N. Howard, and T. P. Williams. 1990. Axial gradients of rhodopsin in light-exposed retinal rods of the toad. *J. Gen. Physiol.* 96:1199–1220.
17. Makino, C. L., and R. L. Dodd. 1996. Multiple visual pigments in a photoreceptor of the salamander retina. *J. Gen. Physiol.* 108:27–34.
18. Govardovskii, V. I., N. Fyhrquist, ..., K. Donner. 2000. In search of the visual pigment template. *Vis. Neurosci.* 17:509–528.
19. Matthews, R. G., R. Hubbard, ..., G. Wald. 1963. Tautomeric forms of metarhodopsin. *J. Gen. Physiol.* 47:215–240.
20. Brown, P. K., I. R. Gibbons, and G. Wald. 1963. The visual cells and visual pigment of the mudpuppy, *Necturus*. *J. Cell Biol.* 19:79–106.
21. Mariani, A. P. 1986. Photoreceptors of the larval tiger salamander retina. *Proc. R. Soc. Lond. B Biol. Sci.* 227:483–492.
22. Hárosi, F. I. 1975. Absorption spectra and linear dichroism of some amphibian photoreceptors. *J. Gen. Physiol.* 66:357–382.
23. Kashiwayanagi, M., A. Suenaga, ..., K. Kurihara. 1990. Membrane fluidity changes of liposomes in response to various odorants. Complexity of membrane composition and variety of adsorption sites for odorants. *Biophys. J.* 58:887–895.
24. Edwards, P. C., J. Li, ..., G. F. Schertler. 2004. Crystals of native and modified bovine rhodopsins and their heavy atom derivatives. *J. Mol. Biol.* 343:1439–1450.
25. Palczewski, K., T. Kumasaka, ..., M. Miyano. 2000. Crystal structure of rhodopsin: a G protein-coupled receptor. *Science.* 289:739–745.
26. Sperling, W., and C. N. Rafferty. 1969. Relationship between absorption spectrum and molecular conformations of 11-*cis*-retinal. *Nature.* 224:590–594.
27. Jin, J., R. K. Crouch, ..., M. C. Cornwall. 1993. Noncovalent occupancy of the retinal-binding pocket of opsin diminishes bleaching adaptation of retinal cones. *Neuron.* 11:513–522.
28. Ala-Laurila, P., M. C. Cornwall, ..., M. Kono. 2009. The action of 11-*cis*-retinol on cone opsins and intact cone photoreceptors. *J. Biol. Chem.* 284:16492–16500.
29. Towner, P., W. Gaertner, ..., H. Hopf. 1981. Regeneration of rhodopsin and bacteriorhodopsin. The role of retinal analogues as inhibitors. *Eur. J. Biochem.* 117:353–359.
30. Crouch, R. K., C. D. Veronee, and M. E. Lacy. 1982. Inhibition of rhodopsin regeneration by cyclohexyl derivatives. *Vision Res.* 22:1451–1456.
31. Sachs, K., D. Maretzki, ..., K. P. Hofmann. 2000. Diffusible ligand all-*trans*-retinal activates opsin via a palmitoylation-dependent mechanism. *J. Biol. Chem.* 275:6189–6194.
32. Jones, G. J., R. K. Crouch, ..., G. J. Chader. 1989. Retinoid requirements for recovery of sensitivity after visual-pigment bleaching in isolated photoreceptors. *Proc. Natl. Acad. Sci. USA.* 86:9606–9610.
33. Andersen, O. S., and R. E. Koeppe, 2nd. 2007. Bilayer thickness and membrane protein function: an energetic perspective. *Annu. Rev. Biophys. Biomol. Struct.* 36:107–130.
34. McIntosh, T. J., and S. A. Simon. 2006. Roles of bilayer material properties in function and distribution of membrane proteins. *Annu. Rev. Biophys. Biomol. Struct.* 35:177–198.
35. Wang, L., B. Martin, ..., S. Maudsley. 2009. Allosteric modulators of G-protein-coupled receptors: future therapeutics for complex physiological disorders. *J. Pharmacol. Exp. Ther.* 331:340–348.
36. Yuan, C., H. Chen, ..., T. G. Ebrey. 1998. The unique lipid composition of gecko (*Gekko Gekko*) photoreceptor outer segment membranes. *Comp. Biochem. Physiol. B Biochem. Mol. Biol.* 120:785–789.
37. Ma, J.-X., S. Znoiko, ..., R. K. Crouch. 2001. A visual pigment expressed in both rod and cone photoreceptors. *Neuron.* 32:451–461.
38. Kefalov, V. J., M. E. Estevez, ..., K. W. Yau. 2005. Breaking the covalent bond—a pigment property that contributes to desensitization in cones. *Neuron.* 46:879–890.
39. Chen, N., J.-X. Ma, ..., R. K. Crouch. 1996. Molecular cloning of a rhodopsin gene from salamander rods. *Invest. Ophthalmol. Vis. Sci.* 37:1907–1913.
40. Xu, L., E. S. Hazard, 3rd, ..., J. Ma. 1998. Molecular cloning of the salamander red and blue cone visual pigments. *Mol. Vis.* 4:10.
41. Edelhoch, H. 1967. Spectroscopic determination of tryptophan and tyrosine in proteins. *Biochemistry.* 6:1948–1954.
42. Gupta, B. D., and T. P. Williams. 1990. Lateral diffusion of visual pigments in toad (*Bufo marinus*) rods and in catfish (*Ictalurus punctatus*) cones. *J. Physiol.* 430:483–496.
43. Makino, C. L., W. R. Taylor, and D. A. Baylor. 1991. Rapid charge movements and photosensitivity of visual pigments in salamander rods and cones. *J. Physiol.* 442:761–780.
44. Okano, T., Y. Fukada, ..., T. Yoshizawa. 1992. Photosensitivities of iodopsin and rhodopsins. *Photochem. Photobiol.* 56:995–1001.
45. Jones, G. J., A. Fein, ..., M. C. Cornwall. 1993. Visual pigment bleaching in isolated salamander retinal cones. Microspectrophotometry and light adaptation. *J. Gen. Physiol.* 102:483–502.
46. Matsumoto, H., F. Tokunaga, and T. Yoshizawa. 1975. Accessibility of the iodopsin chromophore. *Biochim. Biophys. Acta.* 404:300–308.
47. Park, J. H., P. Scheerer, ..., O. P. Ernst. 2008. Crystal structure of the ligand-free G-protein-coupled receptor opsin. *Nature.* 454:183–187.
48. Scheerer, P., J. H. Park, ..., O. P. Ernst. 2008. Crystal structure of opsin in its G-protein-interacting conformation. *Nature.* 455:497–502.
49. Wang, T., and Y. Duan. 2007. Chromophore channeling in the G-protein coupled receptor rhodopsin. *J. Am. Chem. Soc.* 129:6970–6971.
50. Hildebrand, P. W., P. Scheerer, ..., M. Heck. 2009. A ligand channel through the G protein coupled receptor opsin. *PLoS ONE.* 4:e4382.
51. Reuter, T. 1966. The synthesis of photosensitive pigments in the rods of the frog's retina. *Vision Res.* 6:15–38.
52. Dartnall, H. J. A. 1967. The visual pigment of the green rods. *Vision Res.* 7:1–16.
53. Schädell, S. A., M. Heck, ..., K. P. Hofmann. 2003. Ligand channeling within a G-protein-coupled receptor. The entry and exit of retinals in native opsin. *J. Biol. Chem.* 278:24896–24903.
54. Ablonczy, Z., M. Kono, ..., R. K. Crouch. 2006. Palmitoylation of cone opsins. *Vision Res.* 46:4493–4501.
55. Teller, D. C., T. Okada, ..., R. E. Stenkamp. 2001. Advances in determination of a high-resolution three-dimensional structure of rhodopsin, a model of G-protein-coupled receptors (GPCRs). *Biochemistry.* 40:7761–7772.